

Synth-Align: Improving Trustworthiness in Vision-Language Model with Synthetic Preference Data Alignment

Robert Wijaya, Ngoc-Bao Nguyen, Ngai-Man Cheung

Singapore University of Technology and Design
8 Somapah Rd, Singapore 487372

robert_wijaya@mymail.sutd.edu.sg, thibaongoc_nguyen@sutd.edu.sg, ngaiman_cheung@sutd.edu.sg

Abstract

Large Vision-Language Models (LVLMs) have shown promising capabilities in understanding and generating information by integrating both visual and textual data. However, current models are still prone to hallucinations, which degrade the performance and greatly harm the user experience in real-world applications. Post-training alignment, particularly preference-tuning, is intended to align model outputs and behaviors (safety, instruction-following, style), ensuring robustness and adaptability to a wide range of tasks. The use of synthetic data for alignment, particularly in multimodal settings, remains under explored. Existing approaches typically use a strong model or a ground-truth model (CLIP) to determine positive and negative image-text data points. This paper proposes SynthAlign, a pipeline to generate and collect synthetic human-preference image-text data with optimal control built specifically for post-training alignment with DPO. At the core of the framework is the utilization of reward models as a proxy of human preference. A series of evaluation and benchmarking is provided to validate the effectiveness of the proposed framework and the resulting dataset. Notably, our framework enhanced LLaVA-1.5-7B achieved substantial POPE improvements: 87.6% accuracy and 97.8% precision, MMHal-Bench score increased from 2.36 to 3.49, and hallucination rate decreased from 51.0% to 25.0% (a 50.98% relative reduction). The model weights and dataset are available on our Hugging Face page¹.

1 Introduction

Large vision-language models (LVLMs) (Alayrac et al. 2022; Liu et al. 2023, 2024a; He et al. 2024; Zhu et al. 2023; Bai et al. 2023; McKinzie et al. 2024) have shown potential capability in understanding and generating complex information by integrating both visual and textual data, enabling advancement in downstream tasks such as caption generation and visual question answering. Despite the remarkable success, current LVLMs are still facing issue such as confidently providing mislead response in their generated output text that deviates from human preference due to the difference between the pre-training data and the distributions in real user prompts (Sun et al. 2023; Yu et al. 2024c,b). This discrepancy results in several problems, such as the inability to accurately capture all attributes or properties described in the text prompts, and the occasional generation

of content with hallucinated details. While pretraining and supervised fine-tuning are crucial for developing foundational capabilities, post-training alignment, specifically the preference-tuning, has become an essential step before deploying LVLMs to the public to mitigate the risk of generating hallucinate, offensive and misleading content.

It has long been know that higher-quality data leads to better results. Recent work shows high-quality data increase trustworthiness and reduces hallucinations in model outputs (Zhao et al. 2023a; Gunasekar et al. 2023). However, the use of synthetic data for alignment, particularly in multimodal settings, remains under explored. In fact, using synthetic data gives precise control over specific image types, especially in domains where real data is scarce or difficult to obtain. In this work, we go beyond the initial foray of previous works to evaluate if high-quality, carefully curated synthetic (image-text) data could improve the SOTA vision-language models, while manage to reduce the dataset size and training compute.

Following the path of LLM training, reinforcement learning from human feedback (RLHF) (Ouyang et al. 2022; Bai et al. 2022) is a general approach to address the problems. As this technique is expensive, laborious, and also often requiring training a policy model, Direct Preference Optimization (DPO) (Rafailov et al. 2024) is proposed to improve efficiency. This method allow direct training using data obtained either from human preference or powerful LLMs. The existing approach to construct human preference typically using a strong model such as GPT-4o for preference ranking or feedback assessment (Li et al. 2023c; Yu et al. 2024c; Zhao et al. 2023b). However, using this model for generation and ranking is neither scalable nor cost-effective for long-term. Another concurrent work (Ouali et al. 2024) constructs a dataset for DPO training using CLIP scores to generate preference pairs. While their experiments demonstrates significant improvements, we argue that the proposed dataset is relatively large for post-training purpose—which may not that efficient for DPO-based training. Additionally, there is a concern that relying solely on synthesized data, especially if it lacks quality control, can lead to a reduction in data diversity and introduce distortions (Hataya, Bao, and Arai 2023; Shumailov et al. 2023).

To address the aforementioned challenges, we propose a new framework that leverages generative models and pre-trained

¹https://huggingface.co/datasets/pdsdp/synthalign-v1_0-data

reward models as proxies of human preferences. We employ ImageReward (Xu et al. 2024) and Llama-3-8B-ArmoRM scoring model (Wang et al. 2024) to evaluate this synthetic images and their associated responses. When noisy or uncertain data is generated, our oracle, in this case, the reward model with built-in knowledge, acts as a verifier for assessing the quality or correctness of the data. It helps decide which data points are valuable and should be retained for training, enabling us to effectively construct preferred and dispreferred response pairs for DPO training.

Our approach begins by generating synthetic images using Stable Diffusion² from a set of text-to-image prompts. Each generated image is evaluated by a pre-trained reward model, which rate and rank the images based on human preference alignment. The highest-ranked image is selected, and a corresponding instruction prompt is generated for further response generation using open-source LVLMS. The responses are then evaluated using a reward model that assesses helpfulness, correctness, coherence, complexity, and verbosity. The responses with the highest and lowest scores are selected as positive and negative preference data, respectively, which are then used for DPO training. By integrating these generative and reward models into our framework, we significantly reduce the human reliance on human-annotated datasets while maintaining strong alignment with human preference.

To validate the effectiveness of our framework and the resulting dataset, we evaluate our model across various hallucination and vision language benchmarks, demonstrating significant improvement in the trustworthiness and reasoning capabilities of the LVLMS.

The contributions of this paper are summarized as follows:

- We introduce a new pipeline for generating and collecting synthetic human-preference data with optimal control using a pre-trained reward model for a demanding post-training alignment task with DPO.
- We provide a small amount of synthetic human-preference image-text dataset for direct post-training alignment purposes.
- We conduct extensive evaluations on vision-language tasks and hallucination benchmarks to assess the performance of our model, along with some analysis of utilizing synthetic data.

2 Related Works

Large Vision-Language Models. The rapid progress in LVLMS has gained significant attention in recent years, driven by advancements in combining vision and language (Alayrac et al. 2022; Li et al. 2023b; Dai et al. 2023; Zhu et al. 2023; Liu et al. 2023; McKinzie et al. 2024; Bai et al. 2023; Laurençon et al. 2024). A critical factor in the success of both LLMs and LVLMS is the quality of data they are trained on. High-quality curated datasets like those used for LLMs (Liu et al. 2024b; Zhou et al. 2023; Chen et al. 2024b) and LVLMS (He et al. 2024; Wang et al. 2023a) have

been crucial in enhancing language generation and image-text alignment capabilities, respectively. Recent studies have increasingly focused on refining the quality of captions for multimodal datasets to improve model performance, exploring various techniques to optimize caption quality, and emphasizing the crucial role of well-crafted captions in improving multimodal understanding (Chen et al. 2023b, 2024a; Li et al. 2024; Zhao et al. 2023a; Yu et al. 2024a; Lai et al. 2024). Our work builds on these advancements by introducing a new approach that leverages synthetic data and human preference modeling to further enhance the alignment and performance of LVLMS.

Preference Alignment. Aligning human preferences for LVLMS has become an important area of research to mitigate safety and ethical concerns in real-world applications. One of the most prominent approaches is Reinforcement Learning from Human Feedback (RLHF) (Ouyang et al. 2022), where models fine-tuned based on human preferences to better aligned with desired output. Techniques like proximal policy optimization (PPO) (Schulman et al. 2017) and DPO (Rafailov et al. 2024) are typically used to perform this alignment process. Recent studies have applied RLHF to LVLMS such as LLaVA-RLHF (Sun et al. 2023). Follow-up works, such as RLHF-V (Yu et al. 2024b) improve this by collecting human feedback in a more fine-grained form to mitigate hallucination problem in LVLMS. Subsequently, Silkie (Li et al. 2023c) and RLAI-F-V (Yu et al. 2024c) explore the effectiveness of AI feedback with GPT-4 and open-source LVLMS to assess the quality of different model outputs. Recent works have utilized DPO in vision-language tasks (Zhou et al. 2024) and incorporated CLIP for scoring samples (Ouali et al. 2024). While their experiments showed significant improvements, the proposed dataset’s size relatively large. Our resulting dataset comprises only 9K image-text pairs, leveraging a human preference reward model as a proxy for human feedback to ensure higher quality, responsible, and safety alignment in downstream tasks.

3 SynthAlign: Synthetic Preference Data for Post-Training Alignment with DPO

The framework follows a typical DPO-based training pipeline and consists of three key stages: generation, annotation, and optimization. We introduce modifications that leverage generative and reward models; specifically, our approach consists of: (1) image generation and ranking, and (2) response generation and ranking, (3) DPO training. Initiating with a GPT-4-derived prompt, we employ Stable Diffusion to synthesize four different images, each with a different guidance scale. A pre-trained reward model evaluates these images, and we select the highest-scoring one. Subsequently, both the selected image and the initial text-to-image prompt serve as the basis for crafting an instruction prompt. These responses are assessed by a reward model based on helpfulness, correctness, coherence, complexity, and verbosity. The top-scoring response is chosen as positive preference data, and the lowest as negative preference data. Finally, the model undergoes DPO training using Equation 4, as illustrated in Figure 1.

²<https://huggingface.co/stabilityai/stable-diffusion-3-medium>

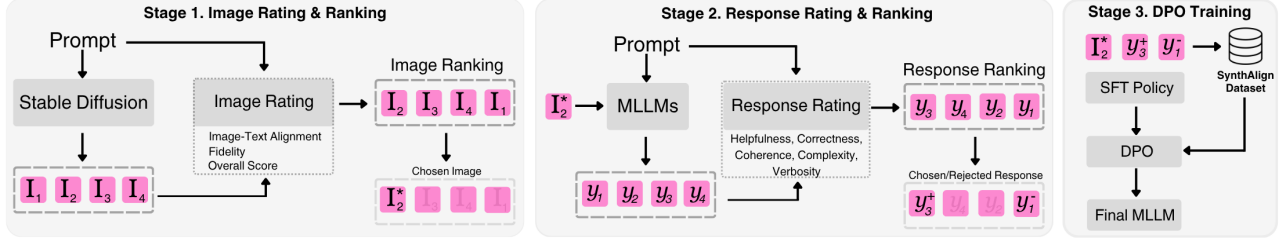


Figure 1: Overview of the framework: Starting with an initial text-to-image prompt, the Stable Diffusion model generates synthetic images. These images are then filtered using a reward model to exclude low-quality samples and retain only those with the highest scores. The selected images, along with their corresponding instruction prompts, serve as input for open-source LVLMs to generate responses. These responses are evaluated based on various criteria, and only the highest-scoring ones are selected to identify the most suitable positive and negative pairs for DPO-based training.

3.1 Background

Direct Preference Optimization. Direct Preference Optimization (DPO) is a framework designed for preference learning, where the goal is to optimize a model’s behavior based on human preferences. The theoretical foundation of DPO is the Bradley-Terry model (Bradley and Terry 1952) that used to quantify how well the learned reward function aligns with the preference data.

We consider a dataset of preference pairs $\mathcal{D}_P = \{x^{(i)}, y_w^{(i)}, y_l^{(i)}\}_{i=1}^N$ where each $x^{(i)}$ represents an input prompt, in this case, a combination of text and images modality, and $y_w^{(i)}$ and $y_l^{(i)}$ denote the preferred and dis-preferred responses to that corresponding to the input x , respectively. The probability that a response y_w is preferred over y_l is given by:

$$P(y_w > y_l) = \sigma(r_\phi(x, y_w) - r_\phi(x, y_l)) \quad (1)$$

This equation reflect the Bradley-Terry model’s assumption that the probability of preferring one response over another depends on the difference in their assigned rewards. The goal is to train a reward function $r_\phi(x, y)$ that assigns higher scores to preferred responses over dis-preferred ones. This can be achieved by minimizing the following loss function.

$$\mathcal{L}_{RM}(\phi) = -\mathbb{E}_{(x, y_w, y_l) \sim \mathcal{D}_P} [\log \sigma(r_\phi(x, y_w) - r_\phi(x, y_l))] \quad (2)$$

where σ denotes the sigmoid function. The next step is we duplicate the policy model π_θ to create a reference model π_{ref} which remains frozen during training. The reference model serves as a baseline, helping to regularize the updated policy and prevent it from deviating too far from the initial model. The overall objective is formulated as follows.

$$\max_{\pi_\theta} \mathbb{E}_{x \sim \mathcal{D}, y \sim \pi_\theta(y|x)} [r_\phi(x, y)] - \beta \mathbb{D}_{KL}[\pi_\theta(y|x) || \pi_{ref}(y|x)] \quad (3)$$

where β is the KL penalty coefficient, and \mathbb{D}_{KL} denotes the Kullback-Leibler divergence between the updated policy π_θ and reference policy π_{ref} . By leveraging the structure of the objective in Equation 3, we can reformulate the optimization as a classification loss over the preferred data, which leads

to the following loss function for DPO.

$$\mathcal{L}_{DPO}(\pi_\theta; \pi_{ref}; \mathcal{D}_P) = -\mathbb{E}_{(x, y_w, y_l) \sim \mathcal{D}_P} \left[\log \sigma \left(\beta \log \frac{\pi_\theta(y_w|x)}{\pi_{ref}(y_w|x)} - \beta \log \frac{\pi_\theta(y_l|x)}{\pi_{ref}(y_l|x)} \right) \right] \quad (4)$$

This loss function transforms the problems into a binary classification task, where the model learns to assign higher probabilities to preferred responses compared to dis-preferred ones.

3.2 Image Generation and Ranking

We utilize GPT-4 to generate text-to-image prompts spanning 10 different topics, including art, school, transport, weather, and daily activities ensuring diversity in content. Let $\mathcal{P} = \{p_1, p_2, \dots, p_n\}$ denote the set of prompts, where p_i represents the i -th prompt in the set. For each prompt p_i , we use Stable Diffusion to generate synthetic images. By adjusting the guidance scale, we generate a set of four images $\mathcal{I}_{p_i} = \{I_1, I_2, I_3, I_4\}$ for each prompt p_i .

Let $I_{p_i}^g$ represent the generated image for prompt p_i with guidance scale g . Formally we can express the image generation as follows:

$$I_{p_i}^g = SD(p_i, g) \quad (5)$$

where g varies for each image to achieve different styles and levels of prompt alignment. This approach helps generate diverse outputs for each prompt while maintain consistency in the generation process. We conduct an analysis specifically on guidance scale (see Section 4.3) to study scale at which the model produces preferable images. To reduce noise and enhance robustness, the generated synthetic images are filtered to remove low-quality samples. An image filtering strategy, serving as a proxy for human preferences, is employed to exclude low-quality images and retain those that are more likely be preferred by humans. Specifically, each image in \mathcal{I}_{p_i} is evaluated using a pre-trained reward model (Xu et al. 2024), denote as $R_{img}(I)$ trained on human feedback to assign quality scores to the synthetic images. The reward model evaluates the images according to criteria such as image-text alignment and fidelity. The score for each image is denoted as follows:

$$s_{I_j} = R_{img}(I_j) \quad (6)$$

where $I_j \in \mathcal{I}_{p_i}$. Images with lower scores are discarded, while image with the highest score is selected as the representative image:

$$I_{p_i}^* = \arg \max_{I_j \in \mathcal{I}_{p_i}} s_{I_j} \quad (7)$$

Unlike CLIP which measures image-text similarity through contrastive alignment, the reward model provides a more nuanced evaluation by considering multiple criteria that reflects human preferences. By integrating reward model as our filtering mechanism, we achieve a higher degree of quality control in image selection. This approach surpasses CLIP’s capabilities in tasks where image quality, fidelity, and nuanced alignment with text prompts are critical for constructing synthetic dataset.

The selection process for generated images involves assigning each image a score by the reward model, with the highest-scoring image being selected. For example, in the second row of Figure 2 (elderly couple feeding ducks), the image generated with a guidance scale of 7.0 received the highest score (2.23), likely due to its alignment with the prompt, where the couple is seated close to the ducks. In contrast, the third image, generated with a guidance scale of 9.0, received the lowest score (-0.18) because it depicts an unrealistic scenario where the elderly couple appears to be standing in the water and does not align well with the prompt description. Similarly, in the third row (metro train crossing a bridge), the first and second images have relatively small score differences (2.08 and 2.15), as both are visually appealing and closely match the prompt’s description of a cityscape with a train, though the second image slightly better captures the intended details of the scene. This evaluation demonstrates how the reward model helps select the most relevant image from multiple outputs, optimizing the use of Stable Diffusion for text-to-image tasks.

3.3 Response Generation and Ranking

Given the selected image $I_{p_i}^*$, we generate a corresponding instruction prompt $q_{p_i}^*$ utilizing GPT-4o. This is accomplished by extracting the relevant information from the original text-to-image prompt and crafting an instruction prompt designed to capture the specific details of the image. This instruction prompt along with the image, is then fed as input to open-source LVLMs, which generate responses $\mathcal{Y}_{p_i} = \{y_1, y_2, y_3, y_4\}$ from different number of LVLMs, including LLaVA-1.6-Mistral-8x7B, LLaVA-1.6-Vicuna-13B, and LLaVA-1.6-Llama-8B, InternVL2.5-8B, and Mini-InternVL-4B. Let the response generation process be represented as follows:

$$\mathcal{Y}_{p_i} = LVLMs(I_{p_i}^*, q_{I_{p_i}^*}) \quad (8)$$

where \mathcal{Y}_{p_i} denotes the set of four generated responses for prompt p_i and the chosen image $I_{p_i}^*$. Each response $y_j \in \mathcal{Y}_{p_i}$ is evaluated by a reward model $R_{resp}(y_j)$, in this case we use Llama-3-8B-ArmoRM (Wang et al. 2024) to produce score of each response based on helpfulness, correctness, coherence, complexity, and verbosity.

$$s_{y_j} = R_{resp}(y_j) \quad (9)$$

Prompt	Stable Diffusion (Guidance: 5.0, 7.0, 9.0, 11.0)			
A warm, sunny day at a lakeside cabin, with the gentle breeze rustling the leaves of the trees, and the sun sparkling off the calm water, as boats drift lazily by.				
An elderly couple feeding ducks at a pond in the park on a calm afternoon.				
A metro train crossing a bridge over a river within the city.				
A ceramic vase with relief carvings of swirling ocean waves, glazed in shades of blue and turquoise.				

Figure 2: The figure illustrates image generation results using Stable Diffusion across four different guidance scales (5.0, 7.0, 9.0, 11.0), with the highest-scored image selected for each prompt based on a preference model evaluation.

The response with the highest score is selected as the positive preference data y^+ , and the response with the lowest score is selected as the negative preference data y^- , denote as follows.

$$y^+ = \arg \max_{y_j \in \mathcal{Y}_{p_i}} s_{y_j}, \quad y^- = \arg \min_{y_j \in \mathcal{Y}_{p_i}} s_{y_j} \quad (10)$$

This expression represents selecting the response y^+ with the highest score and the response y^- with the lowest score. The dispreferred responses highlighted in Figure 3 demonstrate issues such as redundancy, speculative language, and lack of precision. For instance, in the dispreferred response about the vase (top row), unnecessary repetition can reduce clarity, while speculative details in the metro scene (bottom row) reduce reliability and coherence. Conversely, the preferred responses are more concise, focus on key visual elements, and articulate relevant details with precision. The reward model, Llama-3-8B-ArmoRM (Wang et al. 2024), evaluates these characteristics, ensuring the selection of responses that are helpful, accurate, and engaging, improving the overall quality and relevance of the content generated by LVLMs.

3.4 Discussion

Our framework leveraging synthetic data generated through generative models and evaluated using pre-trained reward models as proxies for human preferences. This allows us to effectively filter and select high-quality data for training, addressing issues related to data quality and alignment. Notably, our analysis reveals that our reward models shows significant overlap with methods like CLIP and BLIP

	Preferred Response	Dispreferred Response
 <p>How do the flowing lines and blue-green glaze on the ceramic vase mimic the motion of ocean waves?</p>	<p>The flowing lines and blue-green glaze on the ceramic vase mimic the motion of ocean waves by creating a sense of fluidity and movement. The wavy lines and the glaze's coloration evoke the natural patterns and colors found in the ocean. The glaze's coloration, which includes shades of blue and green, is reminiscent of the colors found in the ocean, while the flowing lines give the impression of the waves' dynamic and ever-changing nature. This artistic representation of ocean waves adds a sense of depth and realism to the vase, making it a captivating piece of art.</p>	<p>The vase is a beautiful piece of art. The glaze on the vase is a blue-green color that mimics the motion of ocean waves. The lines flowing on the vase are designed to look like the waves of the ocean. The glaze is applied in a way that creates a sense of movement and fluidity, giving the vase a dynamic and lively appearance. The artist has skillfully used the glaze to create a realistic representation of the ocean waves, making the vase not only a functional piece of art but also a decorative piece that can enhance the aesthetic appeal of any space it is placed in.</p>
 <p>What views do passengers on a metro train enjoy as it crosses a bridge over a river, with city skyscrapers visible in the distance?</p>	<p>Passengers on the metro train enjoy a scenic view of the city skyline, with the river flowing beneath the bridge. The train is traveling over the bridge, providing a unique perspective of the urban landscape. The city skyscrapers in the distance add to the overall beauty of the scene, creating a sense of connection between the urban environment and the natural element of the river. This view offers a glimpse into the city's architectural and geographical features, making the journey on the metro train a visually engaging experience.</p>	<p>Passengers on a metro train enjoy a variety of views as they cross the bridge over the river. They can see the city skyscrapers in the distance, which provide a sense of the urban environment they are traveling through. As the train approaches the bridge, passengers can observe the river flowing beneath the bridge, and possibly the riverbanks and any greenery or park areas nearby. Once the train is on the bridge, passengers can look out over the river, taking in the view of the water and any boats or watercraft that may be present. Additionally, passengers can enjoy the architectural details of the bridge itself, as well as the cityscape in the background, which may include other bridges, buildings, and possibly some street scenes.</p>

Figure 3: **Sample of preferred and dispreferred responses.** The dispreferred ones include speculative, redundant, or unclear information. This highlights the quality distinctions in vision-language task performance in the context of preference learning.

in selecting optimal images, indicating aligned preferences in image-text alignment and visual quality (See Table 4). However, when we perform LLM-as-a-Judge with stronger model (GPT-4o) in order to select the best image given two images and a caption, the Reward Model (RM) performs better than CLIP in image-text alignment tasks. Out of 100 total comparisons, RM won 53 times, CLIP won 37 times, and there were 10 ties (See Table 5).

4 Experiments

In this section, we conduct evaluations on visual language tasks and hallucination benchmarks, as detailed in Section 4.2. Also, we analyze the effectiveness of synthetic data and the proposed DPO framework, as discussed in Section 4.3.

4.1 Experimental Settings

Implementation Details. In this work, we utilize the LLaVA-1.5 and LLaVA-1.6 architecture, which utilize CLIP vision encoder (Radford et al. 2021). We keep the vision encoder frozen during training. For the LLM, we use the pre-trained Vicuna 7B (Bai et al. 2023) a LoRA (Hu et al. 2021). The models are subsequently fine-tuned for 2 epochs using DPO-based optimization on the curated dataset. We set gradient accumulation steps are set to 4, and learning rate of $1e-5$. Model training is performed using DeepSpeed Zero-2 on $2 \times 80GB$ A100 GPUs.

Evaluation Benchmarks. To assess the performance of our LVLMs, we evaluate them on various vision-language tasks and hallucination benchmarks. For vision language tasks, we adopt VizWiz (Gurari et al. 2018), MMMU (Yue et al. 2024), SEED (Li et al. 2023a), SQA (Lu et al. 2022), MME (Fu et al. 2023), MM-Vet (Yu et al. 2023). Each of these benchmarks contains task that evaluate reasoning, cognition, and perception capabilities of LVLMs. These evaluation results for general vision language tasks are obtained using standardized framework, LMMs Eval (Zhang et al. 2024).

We further evaluate our approach using comprehensive hallucination benchmarks, including Object HalBench

(Rohrbach et al. 2018), AMBER (Wang et al. 2023b), and POPE (Li et al. 2023d). Briefly, Object HalBench is used to assess common object hallucinations in image descriptions; MMHal-Bench asks GPT-4V to compare model outputs with human responses to evaluate response-level hallucination rates and informativeness; and AMBER is an LLM-free, multidimensional benchmark for LVLm hallucination evaluation.

Baselines. We first compare our proposed approach on visual-language tasks proposed approach on visual language tasks with the general-purpose LVLms, including BLIP-2 (Li et al. 2023b), Instruct-BLIP (Dai et al. 2023), Shikra (Chen et al. 2023a), MiniGPT-4 (Zhu et al. 2023), Qwen-VL (Bai et al. 2023), and LLaVA-1.5 (Liu et al. 2024a). Additionally, we assess our model on hallucination benchmarks against other preference-learning LVLms, such as LLaVA-RLHF (Sun et al. 2023), Silkie (Li et al. 2023c), RLHF-V (Yu et al. 2024b), and CLIP-DPO (Ouali et al. 2024).

4.2 Main Results

Evaluation on Visual-Language Tasks and Hallucination Benchmarks. The evaluation results on visual language tasks are reported in Table 2. We observed that our framework sets a new benchmark in vision-language tasks among other open-source models. Notably, our models demonstrate competitive score in several benchmarks, including SQA, MM-Vet, and MMBench. Additionally, the evaluation results on hallucination benchmarks in Table 1 showing improvement in hallucination control and accuracy, particularly reflected in the MMHal-Bench and POPE score.

Qualitative Results. For qualitative results, Figure 4 provides visual examples demonstrating the differences in GPT4-V, and our model outputs. The figure illustrate our model's capability to keep concise and relevance in answer while remains details. Additionally, the comparison highlights how our model able to provide more contextually appropriate response compared to counterparts that tend to generate lengthy answer.

Model	Dataset Size	Feedback	MMHAL-BENCH		AMBER		POPE	
			Score \uparrow	Hall. \downarrow	CHAIR \downarrow	Cover \uparrow	Acc. \uparrow	Pre. \uparrow
Qwen-VL (Bai et al. 2023)			2.76	38.5	6.6	53.2	-	-
GPT4-V		Unspecified	3.49	28.1	4.6	67.1	-	-
LLaVA-RLHF (Sun et al. 2023)	122k	Human	2.02	62.5	9.7	53.2	81.5%	87.2%
LLaVA-1.5-7B (Liu et al. 2024a)			2.36	51.0	7.7	51.6	86.1%	89.1%
+ RLHF-V (Yu et al. 2024b)	1.4k	Human	2.45	51.0	6.3	46.1	86.2%	-
+ Silkie (Li et al. 2023c)	40k	GPT-4V	3.19	32.3	5.4	55.8	83.7%	-
+ POVID (Zhou et al. 2024)	17k	GPT-4V	2.08	56.7	7.4	51.3	86.9%	89.0%
+ RLAI-F-V (Yu et al. 2024c)	16k	MLLM	3.06	29.2	3.0	50.4	81.6%	94.6%
+ CLIP-DPO (Ouali et al. 2024)	750k	CLIP	-	-	3.7	47.8	85.8%	-
+ SynthAlign (ours)	9k	RM	3.49	25.0	7.5	49.7	87.6%	97.8%

Table 1: Hallucination evaluation results on several benchmarks. The inclusion of our approach with LLaVA-1.5-7B models shows performance improvements.

Model	LLM	ScienceQA	MME	VizWiz	MMMU	SEED	MM-Vet
BLIP-2 (Li et al. 2023b)	Vicuna 13B	53.8	290.0	25.3	34.4	49.7	22.4
Instruct-BLIP (Dai et al. 2023)	Vicuna 13B	63.1	291.8	34.5	32.9	57.8	26.2
Shikra (Chen et al. 2023a)	Vicuna 13B	45.8	-	-	-	-	-
MiniGPT-4 (Zhu et al. 2023)	Vicuna 7B	42.8	144.3	-	26.8	47.4	-
Idefics2 (Laurençon et al. 2024)	LLaMA 7B	-	-	35.5	-	44.5	-
Qwen-VL (Bai et al. 2023)	Qwen 7B	67.1	-	35.2	-	62.3	-
Qwen-VL-Chat (Bai et al. 2023)	Vicuna 7B	68.2	360.7	38.9	35.9	65.4	-
Intern-VL-Chat (Chen et al. 2024c)	Vicuna 7B	-	341.1	52.5	39.1	-	-
LLaVA-1.5 (Liu et al. 2024a)	Vicuna 7B	66.8	355.7	50.0	35.9	66.1	31.1
+ SynthAlign-9K (ours)	Vicuna 7B	69.0 ^{+3.3%}	367.5 ^{+3.3%}	55.3 ^{+10.6%}	36.1 ^{+0.6%}	66.3 ^{+0.3%}	34.1 ^{+9.6%}
+ SynthAlign-12K (ours)	Vicuna 7B	69.4 ^{+3.9%}	378.2 ^{+6.3%}	55.2 ^{+10.4%}	36.2 ^{+0.8%}	66.3 ^{+0.3%}	33.4 ^{+7.4%}

Table 2: Performance comparison of LVLMs across general benchmarks. It highlights the improvements achieved by incorporating our method with LLaVA-1.5-7B models.

4.3 Analysis

Preferable Guidance Scale. We observed that adjusting the guidance scale significantly impacts the quality of synthetic data, as determined by the preferences picked by the reward model. As shown in Figure 5, we sampled three image categories: Art, Industrial, and School related images, and found that a guidance scale of 7.0 yielded the highest selection percentages, peaking at around 30%. However, when the guidance scale increased to 11.0, there was a sharp decline in preference, with all categories dropping below 20%, indicating that higher guidance scales may compromise visual coherence. In contrast, a guidance scale of 5.0 produced moderate selection percentages. This highlighting the necessity of carefully choosing the image candidates to improve the overall effectiveness of models trained on this synthetic data.

Highlight the Importance of Synthetic Data. The utilization of synthetic data in our framework plays a crucial role in bridging the gap between model capabilities and real-world applications. By generating a diverse set of image-text pairs using generative models, we can simulate a wide range of scenarios that the LVM might encounter. Despite synthetic sources, we observe broad general benchmark gains on LLaVA-1.5 and hallucination benchmark on a stronger benchmark (LLaVA-1.6). This particularly because synthetic data allows the model to learn from a richer set of examples than what might be available through limited

Model	OBJ.HAL BENCH		POPE	
	CHAIR _s \downarrow	CHAIR _i \downarrow	Acc. \uparrow	Pre. \uparrow
Qwen-VL-Chat-7B	48.2	9.1	87.07%	-
LLaVA-1.5-7B	66.8	12.7	85.90%	89.10%
+ HA-DPO	54.0	14.2	84.90%	90.42%
+ VLFeedback	56.3	11.4	83.72%	-
+ POVID	50.7	15.3	84.77%	89.01%
+ RLHF	54.0	9.3	81.50%	87.20%
+ RLHF-V	44.6	7.9	86.20%	-
+SynthAlign-2K	47.3	35.9	82.10%	96.75%
+SynthAlign-5K	43.7	28.0	84.77%	97.91%
+SynthAlign-7K	42.4	26.7	87.52%	97.02%
+SynthAlign-9K	40.7	24.8	87.62%	97.81%
+SynthAlign-12K	39.0	23.6	88.14%	97.53%
LLaVA-1.6-7B	11.7	6.8	86.5%	95.7%
+ SynthAlign-9K	14.0	8.5	84.9%	96.2%
+ SynthAlign-12K	10.0	5.9	86.6%	94.9%

Table 3: Comparison of hallucination evaluation results on Obj.Hal Bench and POPE on various models, and size of the synthetic dataset.

human-annotated datasets. In other words, using synthetic data allows precise control over specific image types or scenarios, especially in domains where real data is scarce or difficult to obtain. We experiment with different dataset setups to highlight the effectiveness of synthetic data. Specifically, we sample our dataset at different sizes ranging from 2K to 12K and measure the model’s hallucination rate after train-

Visual input example



User:
Compare the two surfboards in the photo.

GPT4-V In the photo, you have two surfboards with distinct designs and features:
Top Surfboard: This board has a natural wood finish and features a simpler, more traditional design
Bottom Surfboard: This board is more vibrant with a red base and a detailed geometric
 Overall, the top surfboard seems better suited for traditional surfing styles and possibly.... 1,000 more characters.

LLaVA-1.5 +PDS-DPO The two surfboards in the photo have different designs and colors, making them easily distinguishable from each other. The first surfboard is predominantly red and features a patterned design, while the second surfboard is predominantly white and has a more minimalist design. The contrasting colors and patterns on the surfboards give them a unique and personalized appearance, reflecting the preferences and style of their respective owners.

Figure 4: Qualitative demonstrations comparing our method with GPT4-V.

ing on each sample. The results shown in Table 3 indicate that as the size of the dataset increases, the performance improves accordingly, demonstrating the effectiveness of our framework. This also highlights that carefully constructed and selected synthetic data can benefit model training, while manage to reduce the dataset size and training compute.

Issue on Synthetic Data. In general, relying on synthesised data without careful quality control can lead to reduction in data diversity and introduce distortions. In addition, despite the benefits of using synthetic data, it often fails to capture the full complexity and nuances of real-world scenarios. The quality of generated images remains limited, sometimes producing imprecise or unrealistic visuals. Furthermore, responses generated by current SOTA open-source LLMs can be noisy, containing errors or irrelevant information. Any biases inherent in the generative models may be propagated or even amplified in the synthetic data, negatively affecting the LLM’s fairness and reliability. Therefore, it is crucial to carefully curate and validate synthetic datasets to ensure they contribute positively to the model’s training. When feasible, manual human evaluation may still be necessary to guarantee dataset quality.

Reward Model vs Ground-Truth Scoring Model. We specifically analyze which model is more in line with the reward model by examining the overlap between images selected by different common methods, such as CLIP and BLIP, and examine whether they agree on the best image for a given prompt. Table 4 shows the percentage of common image selections among method pairs, where the Top 1 indicates the highest-ranked image agreed upon, Top 2 includes the top two shared images, and Top 3 covers the top three im-

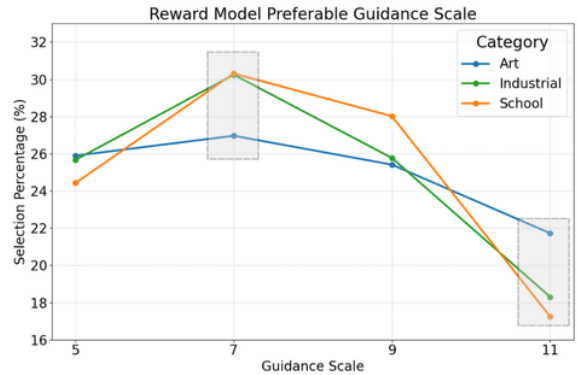


Figure 5: Selection percentage of preferred guidance scales by the reward model.

ages. The reward model is most in line with CLIP, showing the highest common selection percentages of 36.8% at Top 1, 59.5% at Top 2, and 79.13% at Top 3 compared to other method pairs. Reward model and BLIP also show a high degree of overlap, with 31.8% at Top 1 and 77.4% at Top 3, indicating that reward model captures not only image-text alignment but also aspects of visual quality that BLIP may prioritize.

Method Pair	COMMON SELECTION (%)		
	@ Top 1	@ Top 2	@ Top 3
Reward Model & CLIP	36.8	59.5	79.13
Reward Model & BLIP	31.8	53.6	77.40
CLIP & BLIP	28.6	55.9	76.53
All 3 Methods	11.8	34.2	61.87

Table 4: Percentage of common image selections among Reward Model, CLIP, and BLIP.

Outcome	Count	Win Rate (%)
RM Wins	53	58.9%
CLIP Wins	37	41.1%
Ties	10	10%

Table 5: LLM-as-a-Judge (GPT-4o) outcomes with counts, win rates for CLIP and Reward Model.

5 Conclusion

In this work, we attempt vision-language post-training alignment with synthetic human-preference (image-text) data with DPO. At the core of the proposed framework is the utilization of reward models as a proxy for human preference to rate and rank the generated images and text, and hence select only the highest-rated images and text. Our experiments demonstrate favorable improvements in trustworthiness and reasoning capabilities across hallucination benchmarks and vision-language tasks, offering an efficient solution for safer LLM deployment.

References

- Alayrac, J.-B.; Donahue, J.; Luc, P.; Miech, A.; Barr, I.; Hasson, Y.; Lenc, K.; Mensch, A.; Millican, K.; Reynolds, M.; Ring, R.; Rutherford, E.; Cabi, S.; Han, T.; Gong, Z.; Samangooei, S.; Monteiro, M.; Menick, J.; Borgeaud, S.; Brock, A.; Nematzadeh, A.; Sharifzadeh, S.; Binkowski, M.; Barreira, R.; Vinyals, O.; Zisserman, A.; and Simonyan, K. 2022. Flamingo: a Visual Language Model for Few-Shot Learning. In *NeurIPS*.
- Bai, J.; Bai, S.; Yang, S.; Wang, S.; Tan, S.; Wang, P.; Lin, J.; Zhou, C.; and Zhou, J. 2023. Qwen-VL: A Versatile Vision-Language Model for Understanding, Localization, Text Reading, and Beyond. *arXiv preprint arXiv:2308.12966*.
- Bai, Y.; Kadavath, S.; Kundu, S.; Askell, A.; Kernion, J.; Jones, A.; Chen, A.; Goldie, A.; Mirhoseini, A.; McKinnon, C.; et al. 2022. Constitutional ai: Harmlessness from ai feedback. *arXiv preprint arXiv:2212.08073*.
- Bradley, R. A.; and Terry, M. E. 1952. Rank analysis of incomplete block designs: I. The method of paired comparisons. *Biometrika*, 39(3/4): 324–345.
- Chen, G. H.; Chen, S.; Zhang, R.; Chen, J.; Wu, X.; Zhang, Z.; Chen, Z.; Li, J.; Wan, X.; and Wang, B. 2024a. ALLaVA: Harnessing GPT4V-synthesized Data for A Lite Vision-Language Model. *arXiv Preprint arXiv: 2402.11684*.
- Chen, K.; Zhang, Z.; Zeng, W.; Zhang, R.; Zhu, F.; and Zhao, R. 2023a. Shikra: Unleashing Multimodal LLM’s Referential Dialogue Magic. *arXiv preprint arXiv:2306.15195*.
- Chen, L.; Li, J.; Dong, X.; Zhang, P.; He, C.; Wang, J.; Zhao, F.; and Lin, D. 2023b. ShareGPT4V: Improving Large Multi-Modal Models with Better Captions. In *ECCV*.
- Chen, L.; Li, S.; Yan, J.; Wang, H.; Gunaratna, K.; Yadav, V.; Tang, Z.; Srinivasan, V.; Zhou, T.; Huang, H.; and Jin, H. 2024b. AlpaGasus: Training A Better Alpaca with Fewer Data. In *ICLR*.
- Chen, Z.; Wu, J.; Wang, W.; Su, W.; Chen, G.; Xing, S.; Zhong, M.; Zhang, Q.; Zhu, X.; Lu, L.; et al. 2024c. Internvl: Scaling up vision foundation models and aligning for generic visual-linguistic tasks. In *Proceedings of the IEEE/CVF conference on computer vision and pattern recognition*, 24185–24198.
- Dai, W.; Li, J.; Li, D.; Tiong, A. M. H.; Zhao, J.; Wang, W.; Li, B.; Fung, P.; and Hoi, S. 2023. InstructBLIP: Towards General-purpose Vision-Language Models with Instruction Tuning. In *NeurIPS*.
- Fu, C.; Chen, P.; Shen, Y.; Qin, Y.; Zhang, M.; Lin, X.; Yang, J.; Zheng, X.; Li, K.; Sun, X.; et al. 2023. MME: A Comprehensive Evaluation Benchmark for Multimodal Large Language Models. *arXiv preprint arXiv:2306.13394*.
- Gunasekar, S.; Zhang, Y.; Aneja, J.; Mendes, C. C. T.; Del Giorno, A.; Gopi, S.; Javaheripi, M.; Kauffmann, P.; de Rosa, G.; Saarikivi, O.; et al. 2023. Textbooks are all you need. *arXiv preprint arXiv:2306.11644*.
- Gurari, D.; Li, Q.; Stangl, A. J.; Guo, A.; Lin, C.; Grauman, K.; Luo, J.; and Bigham, J. P. 2018. Vizwiz grand challenge: Answering visual questions from blind people. In *Proceedings of the IEEE conference on computer vision and pattern recognition*, 3608–3617.
- Hataya, R.; Bao, H.; and Arai, H. 2023. Will Large-scale Generative Models Corrupt Future Datasets? In *ICCV*, 20555–20565.
- He, M.; Liu, Y.; Wu, B.; Yuan, J.; Wang, Y.; Huang, T.; and Zhao, B. 2024. Efficient Multimodal Learning from Data-centric Perspective. *arXiv Preprint arXiv: 2402.11530*.
- Hu, E. J.; Shen, Y.; Wallis, P.; Allen-Zhu, Z.; Li, Y.; Wang, S.; Wang, L.; and Chen, W. 2021. Lora: Low-rank adaptation of large language models. *arXiv preprint arXiv:2106.09685*.
- Lai, Z.; Zhang, H.; Zhang, B.; Wu, W.; Bai, H.; Timofeev, A.; Du, X.; Gan, Z.; Shan, J.; Chuah, C.-N.; Yang, Y.; and Cao, M. 2024. VeCLIP: Improving CLIP Training via Visual-enriched Captions. In *ECCV*.
- Laurençon, H.; Tronchon, L.; Cord, M.; and Sanh, V. 2024. What matters when building vision-language models? *arXiv preprint arXiv:2405.02246*.
- Li, B.; Wang, R.; Wang, G.; Ge, Y.; Ge, Y.; and Shan, Y. 2023a. Seed-bench: Benchmarking multimodal llms with generative comprehension. *arXiv preprint arXiv:2307.16125*.
- Li, J.; Li, D.; Savarese, S.; and Hoi, S. 2023b. BLIP-2: Bootstrapping Language-Image Pre-training with Frozen Image Encoders and Large Language Models. In *ICML*.
- Li, L.; Xie, Z.; Li, M.; Chen, S.; Wang, P.; Chen, L.; Yang, Y.; Wang, B.; and Kong, L. 2023c. Silkie: Preference Distillation for Large Visual Language Models. *arXiv preprint arXiv:2312.10665*.
- Li, X.; Tu, H.; Hui, M.; Wang, Z.; Zhao, B.; Xiao, J.; Ren, S.; Mei, J.; Liu, Q.; Zheng, H.; Zhou, Y.; and Xie, C. 2024. What If We Recaption Billions of Web Images with LLaMA-3? *arXiv preprint arXiv:2406.08478*.
- Li, Y.; Du, Y.; Zhou, K.; Wang, J.; Zhao, W. X.; and Wen, J.-R. 2023d. Evaluating object hallucination in large vision-language models. *arXiv preprint arXiv:2305.10355*.
- Liu, H.; Li, C.; Li, Y.; and Lee, Y. J. 2024a. Improved baselines with visual instruction tuning. In *CVPR*, 26296–26306.
- Liu, H.; Li, C.; Wu, Q.; and Lee, Y. J. 2023. Visual Instruction Tuning. In *NeurIPS*.
- Liu, W.; Zeng, W.; He, K.; Jiang, Y.; and He, J. 2024b. What Makes Good Data for Alignment? A Comprehensive Study of Automatic Data Selection in Instruction Tuning. In *ICLR*.
- Lu, P.; Mishra, S.; Xia, T.; Qiu, L.; Chang, K.-W.; Zhu, S.-C.; Tafjord, O.; Clark, P.; and Kalyan, A. 2022. Learn to explain: Multimodal reasoning via thought chains for science question answering. *NeurIPS*, 35: 2507–2521.
- McKinzie, B.; Gan, Z.; Fauconnier, J.-P.; Dodge, S.; Zhang, B.; Dufter, P.; Shah, D.; Du, X.; Peng, F.; Weers, F.; et al. 2024. Mm1: Methods, analysis & insights from multimodal llm pre-training. *arXiv preprint arXiv:2403.09611*.
- Ouali, Y.; Bulat, A.; Martinez, B.; and Tzimiropoulos, G. 2024. CLIP-DPO: Vision-Language Models as a Source of Preference for Fixing Hallucinations in LVLMS.

- Ouyang, L.; Wu, J.; Jiang, X.; Almeida, D.; Wainwright, C.; Mishkin, P.; Zhang, C.; Agarwal, S.; Slama, K.; Ray, A.; et al. 2022. Training language models to follow instructions with human feedback. *NeurIPS*, 35: 27730–27744.
- Radford, A.; Kim, J. W.; Hallacy, C.; Ramesh, A.; Goh, G.; Agarwal, S.; Sastry, G.; Askell, A.; Mishkin, P.; Clark, J.; Krueger, G.; and Sutskever, I. 2021. Learning Transferable Visual Models From Natural Language Supervision. *arXiv preprint arXiv:2103.00020*.
- Rafailov, R.; Sharma, A.; Mitchell, E.; Manning, C. D.; Ermon, S.; and Finn, C. 2024. Direct preference optimization: Your language model is secretly a reward model. volume 36.
- Rohrbach, A.; Hendricks, L. A.; Burns, K.; Darrell, T.; and Saenko, K. 2018. Object hallucination in image captioning. *arXiv preprint arXiv:1809.02156*.
- Schulman, J.; Wolski, F.; Dhariwal, P.; Radford, A.; and Klimov, O. 2017. Proximal policy optimization algorithms. *arXiv preprint arXiv:1707.06347*.
- Shumailov, I.; Shumaylov, Z.; Zhao, Y.; Gal, Y.; Papernot, N.; and Anderson, R. 2023. The curse of recursion: Training on generated data makes models forget. *arXiv preprint arXiv:2305.17493*.
- Sun, Z.; Shen, S.; Cao, S.; Liu, H.; Li, C.; Shen, Y.; Gan, C.; Gui, L.-Y.; Wang, Y.-X.; Yang, Y.; et al. 2023. Aligning large multimodal models with factually augmented rlhf. *arXiv preprint arXiv:2309.14525*.
- Wang, A. J.; Lin, K. Q.; Zhang, D. J.; Lei, S. W.; and Shou, M. Z. 2023a. Too Large; Data Reduction for Vision-Language Pre-Training. In *ICCV*.
- Wang, H.; Xiong, W.; Xie, T.; Zhao, H.; and Zhang, T. 2024. Interpretable Preferences via Multi-Objective Reward Modeling and Mixture-of-Experts. *arXiv preprint arXiv:2406.12845*.
- Wang, J.; Wang, Y.; Xu, G.; Zhang, J.; Gu, Y.; Jia, H.; Yan, M.; Zhang, J.; and Sang, J. 2023b. An LLM-free Multi-dimensional Benchmark for MLLMs Hallucination Evaluation. *arXiv preprint arXiv:2311.07397*.
- Xu, J.; Liu, X.; Wu, Y.; Tong, Y.; Li, Q.; Ding, M.; Tang, J.; and Dong, Y. 2024. Imagereward: Learning and evaluating human preferences for text-to-image generation. *NeurIPS*, 36.
- Yu, Q.; Sun, Q.; Zhang, X.; Cui, Y.; Zhang, F.; Cao, Y.; Wang, X.; and Liu, J. 2024a. CapsFusion: Rethinking Image-Text Data at Scale. In *CVPR*.
- Yu, T.; Yao, Y.; Zhang, H.; He, T.; Han, Y.; Cui, G.; Hu, J.; Liu, Z.; Zheng, H.-T.; Sun, M.; et al. 2024b. Rlhf-v: Towards trustworthy mllms via behavior alignment from fine-grained correctional human feedback. In *CVPR*, 13807–13816.
- Yu, T.; Zhang, H.; Yao, Y.; Dang, Y.; Chen, D.; Lu, X.; Cui, G.; He, T.; Liu, Z.; Chua, T.-S.; et al. 2024c. Rlaif-v: Aligning mllms through open-source ai feedback for super gpt-4v trustworthiness. *arXiv preprint arXiv:2405.17220*.
- Yu, W.; Yang, Z.; Li, L.; Wang, J.; Lin, K.; Liu, Z.; Wang, X.; and Wang, L. 2023. Mm-vet: Evaluating large multimodal models for integrated capabilities. *arXiv preprint arXiv:2308.02490*.
- Yue, X.; Ni, Y.; Zhang, K.; Zheng, T.; Liu, R.; Zhang, G.; Stevens, S.; Jiang, D.; Ren, W.; Sun, Y.; et al. 2024. Mmmu: A massive multi-discipline multimodal understanding and reasoning benchmark for expert agi. In *Proceedings of the IEEE/CVF Conference on Computer Vision and Pattern Recognition*, 9556–9567.
- Zhang, K.; Li, B.; Zhang, P.; Pu, F.; Cahyono, J. A.; Hu, K.; Liu, S.; Zhang, Y.; Yang, J.; Li, C.; and Liu, Z. 2024. LMMs-Eval: Reality Check on the Evaluation of Large Multimodal Models. *arXiv preprint arXiv:2407.12772*.
- Zhao, B.; Wu, B.; He, M.; and Huang, T. 2023a. SVIT: Scaling up Visual Instruction Tuning. *arXiv preprint arXiv:2307.04087*.
- Zhao, Z.; Wang, B.; Ouyang, L.; Dong, X.; Wang, J.; and He, C. 2023b. Beyond Hallucinations: Enhancing LVLMS through Hallucination-Aware Direct Preference Optimization. *arXiv:2311.16839*.
- Zhou, C.; Liu, P.; Xu, P.; Iyer, S.; Sun, J.; Mao, Y.; Ma, X.; Efrat, A.; Yu, P.; Yu, L.; Zhang, S.; Ghosh, G.; Lewis, M.; Zettlemoyer, L.; and Levy, O. 2023. LIMA: Less Is More for Alignment. In *NeurIPS*.
- Zhou, Y.; Cui, C.; Rafailov, R.; Finn, C.; and Yao, H. 2024. Aligning modalities in vision large language models via preference fine-tuning. *arXiv preprint arXiv:2402.11411*.
- Zhu, D.; Chen, J.; Shen, X.; Li, X.; and Elhoseiny, M. 2023. MiniGPT-4: Enhancing Vision-Language Understanding with Advanced Large Language Models. In *ICLR*.